

Discriminant Analysis Based Graph for Feature Extraction and Classification of Polarimetric SAR Images

Fatemeh Saneipour^{1*}, Maryam Imani², Hassan Ghassemian³

^{1,2,3} Image processing and Information Analysis Lab, Faculty of Electrical and Computer Engineering, Tarbiat Modares University, Tehran, Iran

¹ f.saneipour@modares.ac.ir

² maryam.imani@modares.ac.ir

³ ghassemi@modares.ac.ir

Keywords—polarimetric synthetic aperture radar (PolSAR), feature extraction, graph, classification.

Abstract

Polarimetric Synthetic Aperture Radar (PolSAR) imagery, as an advanced remote sensing technology provides rich information about the scattering characteristics of the Earth's surface, significantly enhancing classification accuracy. However, effectively integrating contextual features with polarimetric ones remains a key challenge. In this paper, we propose a framework for PolSAR image classification that leverages graph modeling to capture spatial relationships and utilizes the scattering characteristics with physical interpretability of polarimetric data. The proposed method begins with superpixel segmentation to reduce computational complexity and maintain spatial homogeneity. Then, superpixels construct the graph nodes. To enhance class separability, we suggest a superpixel based discriminant analysis transformation to compute the weight matrix used in the graph propagation. Unlike deep learning approaches that learn weights through complex neural networks, our method uses the discriminant analysis based projection to derive the weight matrix in a physically interpretable and computationally efficient manner. The graph based projection results in spatial-polarimetric features that encode both structural and discriminative information. In parallel, we extract another set of polarimetric features from the H-A-Alpha (Cloude-Pottier) decomposition describing the physical scattering mechanisms. The final classification is performed by fusing the graph-derived features and the decomposition-based features and feeding them into a standard classifier such as support vector machine.

1. Introduction

One of the best remote sensing sources for land cover classification is Synthetic Aperture Radar (SAR) image. Polarimetric SAR (POLSAR) images include the polarimetric and scattering characteristics which improve the class separability. In a POLSAR image classification, pre-processing, selecting and extracting appropriate features are crucial steps. Different classic machine learning and deep learning methods have been used to this end. Polarimetric Synthetic Aperture Radar (PolSAR) is an advanced remote sensing technique that emits electromagnetic pulses and captures their backscattered signals, enabling reliable observation regardless of lighting or atmospheric conditions. Unlike conventional SAR systems, PolSAR captures data across multiple polarization channels, leveraging the full vector nature of electromagnetic waves to reveal richer physical and structural details of the observed scene. Owing to its enhanced discriminative capability, this technology has become instrumental in diverse applications, including land-use mapping, environmental monitoring, and urban development planning (Alkhatib, 2025). In (Bdiri, 2024), an unsupervised classification framework is presented for high-resolution multilook PolSAR imagery by fusing a Bayesian nonparametric Dirichlet process mixture model with a Markov random field. The approach automatically infers the number of land-cover classes from the data while models PolSAR statistics via the product model (Wishart speckle and inverse-gamma texture).

The GLCM (Gray-Level Co-occurrence Matrix) method is typically suitable for grayscale images and is widely used for extracting textural features. The Pol+GLCM method extends this approach by incorporating both textural and polarimetric features. By combining these two types of information, Pol+GLCM enhances the accuracy of classification, making it particularly effective for land cover

classification of polarimetric SAR (Synthetic Aperture Radar) imagery. Gabor filters exhibit high capability in pattern and texture recognition within images. These filters are a combination of Gaussian functions and sinusoidal wave functions, allowing them to simultaneously capture spatial and frequency domain characteristics. Gabor filters are commonly applied at multiple orientations and frequencies to extract more detailed and robust textural information from images. In the POL+Gabor method, polarimetric features are first extracted from the image, and then Gabor filters are applied to these features. This integration enables the extraction of textural information from polarimetric data, improving both classification accuracy and pattern recognition performance (Imani, 2021).

Local Energy and Intensity Features (LE-IF) focuses on analyzing local characteristics of an image. These features examine the information surrounding each pixel, enabling an effective description of texture and spatial patterns. LE-IF considers two key aspects: local energy and local intensity. Local energy refers to the sum of pixel values within a specific neighborhood, reflecting the total activity or variation in that region. Local intensity typically refers to the average or maximum pixel value in the local area, indicating the brightness or strength of the signal. These features contribute to a better understanding of texture and object shapes in the image, enhancing the discriminative power in classification tasks. The CLPP-Gabor method is a hybrid approach that combines polarimetric features with textural features extracted using Gabor filters. By fusing polarimetric scattering information with detailed texture descriptors, CLPP-Gabor achieves higher classification accuracy. This synergy allows the method to leverage both the physical scattering properties of different land cover types and their spatial textural patterns, leading to more reliable and precise classification results (Imani, 2021).

* Corresponding author

In (Saneipour, 2024), weighting was used for some methods like maximum likelihood (ML), support vector machine (SVM) and K nearest neighbor (KNN). Some parameters like variance and mean for each feature were used for this weighting. Early efforts in spectral graph theory laid the mathematical groundwork for processing signals on irregular domains, enabling the extension of classical Fourier analysis to graph-structured data through eigen-decomposition of the graph Laplacian (Bharaneswari, 2015).

A foundational framework for semi-supervised learning on graphs leveraged label propagation, where unlabeled nodes inherit predictions based on smoothness assumptions over the underlying manifold (Chitroub, 2004). Researchers introduced a scalable approach to node classification by designing efficient random-walk-based embeddings that capture local neighborhood structures without explicit graph convolutions (Imani, 2022).

One study reformulated convolution operations in the spectral domain using graph Fourier transforms, though it suffered from high computational cost due to full eigendecomposition (Huang, 2020). A parameterized spectral filter was proposed to approximate graph convolutions with Chebyshev polynomials, significantly reducing complexity while preserving localization properties (Zhang, 2023).

The concept of graph coarsening was explored to enable hierarchical learning, mimicking multi-scale analysis in classical signal processing for large-scale network data (Imani, 2022). A method combining manifold learning with discriminant analysis was developed to enhance class separation in low-dimensional subspaces derived from neighborhood graphs (Ni, 2021).

An unsupervised feature learning strategy utilized autoencoders adapted to graph topologies, reconstructing node attributes while preserving adjacency relationships (Wang, 2019). The work on locality-preserving projections extended classical linear discriminant analysis (LDA) by incorporating graph-based similarity to maintain intrinsic geometric structure during dimensionality reduction (Wang, 2022). A transductive inference model employed iterative label diffusion constrained by graph edges, achieving strong performance with minimal labeled examples in citation networks (Nie, 2021).

Researchers have designed a deep architecture stacking graph filters with nonlinearities, though early versions lacked mechanisms to prevent over-smoothing across layers (Sharma, 2021). A study investigated the role of self-loops and degree normalization in stabilizing message passing, leading to more robust aggregation in heterogeneous graphs (Guo, 2022).

An approach integrating Gabor filters with polarimetric features was applied to remote sensing imagery, demonstrating improved texture discrimination in land-cover classification (Wang, 2022). Texture analysis via gray-level co-occurrence matrices was enhanced by coupling with graph-based regularization to enforce spatial consistency in segmentation tasks (Cao, 2023).

A hybrid model fused handcrafted descriptors with graph Laplacian constraints, achieving competitive results without end-to-end training in limited-data regimes (Zhang, 2023). The work on class-wise local preserving projections introduced discriminative graph construction where intra-class compactness and inter-class separation were explicitly optimized (Yin, 2023). Recent advances have combined manifold pursuit with subspace learning to extract low-dimensional representations that respect both local geometry and global class structure (Imani, 2022).

In this paper, a PolSAR image classification method is proposed which models the image through a graph constructed based on superpixels. The projection matrix in the graph propagation rule is obtained by discriminant analysis to maximize the class separability. In addition to extraction of structural and spatial features by the graph based projection, the scattering features extracted by H-A-alpha decomposition are also used for PolSAR image classification using the support vector machine (SVM).

2. Proposed Method

Block diagram of the proposed method is shown in Fig. 1. In one path, the contextual and structural features are explored based on superpixel based graph transformation and in another path, the scattering features are explored. Then, fusion of both graph and scattering features are given to the SVM classifier. The main novelties of the proposed method are represented as follows:

- 1) Development of regularized discriminant analysis method based on superpixel computations.
- 2) The use of discriminant analysis projection in the graph propagation rule.
- 3) Fusion of scattering features with graph based structural features for PolSAR image classification.

2.1. Superpixel Generation

In first step for segmenting the PolSAR image into superpixels the Principal Component Analysis (PCA) is applied. Then, the Simple Linear Iterative Clustering (SLIC) algorithm is used to generate superpixels. This process reduces computational complexity, mitigates noise, and preserves spatial information. Each superpixel represents a homogeneous region in the image. Nine features derived from the Coherence Matrix T are used as input features for each superpixel. These features capture the polarimetric characteristics of the image. The average pixel values within each superpixel are computed and assigned to represent the superpixel's features.

2.2. Graph Modeling

Each superpixel is treated as a node in the graph. The similarity between nodes is measured using the logarithm of normalized inner product of their feature vectors:

$$A(i, j) = \log\left(\frac{x_i \cdot x_j}{\|x_i\| \|x_j\|}\right) \quad (1)$$

To propagate information across the graph, a weight matrix W is computed using the Regularized LDA (RLDA). Unlike many existing methods such as graph convolutional network (GCN) (Mou, 2020) which try to learn weights in a training process through a neural network, here RLDA is used to provide the projection weights. RLDA leverages class labels and scatter matrices to maximize inter-class scattering and minimize the intra-class scattering, which leads to class separability enhancement. Within-Class Scatter Matrix (S_w) and Between-Class Scatter Matrix (S_b) are calculated:

$$S_w = \sum_c \sum_{x_i \in c} (x_i - \mu_c)(x_i - \mu_c)^T \quad (2)$$

$$S_b = \sum_c N_c (\mu_c - \mu)(\mu_c - \mu)^T \quad (3)$$

where μ is the mean of all training samples, μ_i denotes mean of training samples of class number i , N_c is the number of training samples

belonging to class c that c is the number of classes. So, the summation is performed over all available classes.

To provide the discriminant analysis based projection matrix, the projection vectors are obtained by solving the following optimization problem:

$$w = \arg \max_w \frac{w^T S_b w}{w^T S_w w} \quad (4)$$

In contrast to GCN, which is a deep learning based method and uses the learning approach to find the projection weights for the graph propagation, here the RLDA projection is used as the projection matrix

to extract graph features according to the following propagation rule inspired from the GCN:

$$y = A_N X W \quad (5)$$

A_N is the normalize version of the adjacency matrix A computed as follow:

$$A_N = D^{-\frac{1}{2}} A D^{-\frac{1}{2}} \quad (6)$$

where D is the degree matrix of A .

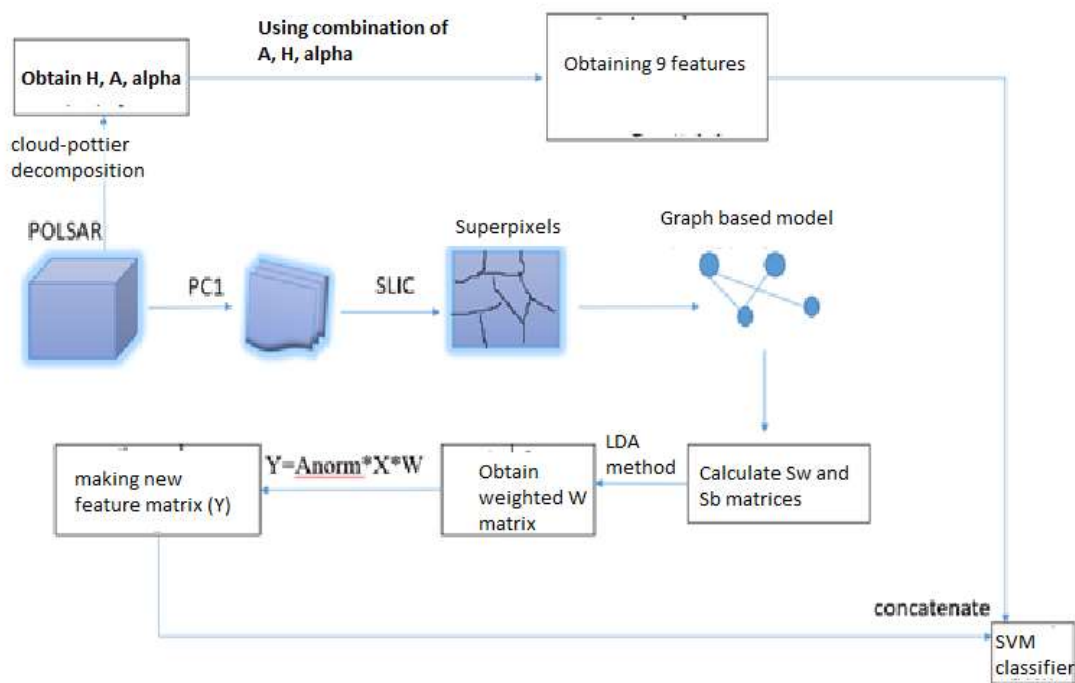


Fig 1. Block diagram of the Proposed Method.

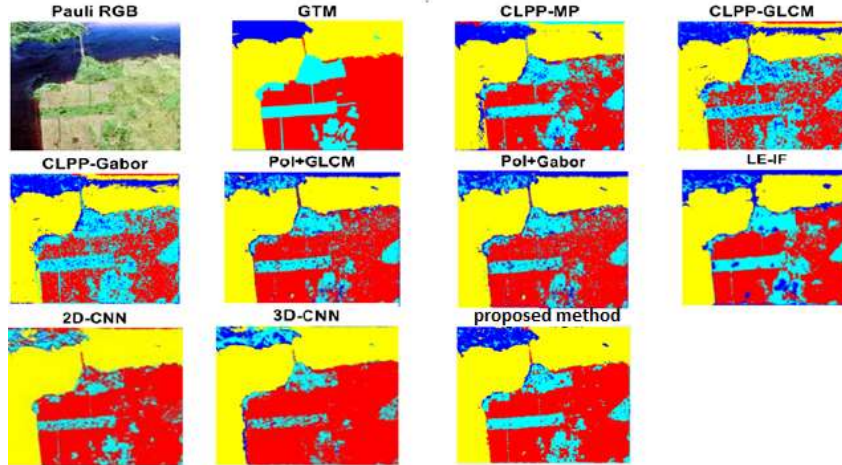


Fig 2. San Francisco classification maps obtained by different methods compared to the proposed method.

2.3. Cloud-pottier features and classification

After Graph based feature extracting, we use cloud-pottier method for scattering feature extraction. Their formulation are represented as follows:

$$P_i = \frac{\lambda_i}{\sum_{k=1}^3 \lambda_k} \quad (7)$$

$$H = -\sum_{i=1}^3 P_i \log_3(P_i) \quad (8)$$

$$A = \frac{\lambda_2 - \lambda_3}{\lambda_2 + \lambda_3} \quad (9)$$

$$\alpha = \sum_{i=1}^3 P_i \alpha_i \quad (10)$$

where λ_i are eigenvalues of the coherency matrix, P_i represent the relative contribution or weight of each scattering mechanism associated with the corresponding eigenvector, H is isotropy, A is anisotropy and α is average scattering alpha angle.

Here, we use H, A and alpha and different combinations of them as the scattering features as follows:

The graph features are fused with the scattering features and then, the fused features are given to the SVM classifier to provide the classification map

3. Experimental results

In this section, the experiments are done on the San Francisco and Flevoland datasets. San Francisco is a C-band, Fully Polarimetric SAR (PolSAR) of 1800×1380 pixels with 4 classes. Flevoland is an L-band AIRSAR image composed of 750×1024 pixels with 15 classes.

The accuracy and validity of each class, and overall accuracy (OA) are used to evaluate the classification performance. All the experiments are performed on an Intel Core i7 CPU, and all codes are written with MATLAB (2017b) development environment.

3.1. Classification results using San Francisco dataset

The results of the proposed method are represented in Table 1. Comparison with other methods have reported in Table 3 and shown in Fig. 2.

The Overall Accuracy of the proposed method is 83%, which is the highest among all reported methods. Compared to deep learning-based approaches like 3D-CNN (88% average accuracy, and 91% overall accuracy) and 2D-CNN (84% overall accuracy), the proposed method achieves comparable or even superior overall accuracy (83% vs. 84% for 2D-CNN) without relying on complex neural architectures.

Name of class	validity	accuracy
mountains	0.86	0.85
green	0.74	0.72
water	0.97	0.99
buildings	0.92	0.92
overall	0.88	0.88

Table 1. Classification results of the proposed method for San Francisco dataset.

3.2. Classification results using Flevoland dataset

The result of this method has shown in Table 2. This method is compared to other methods and results are shown in Fig. 3 and Table 4. The proposed method, significantly outperforms other machine learning methods and also deep learning-based approaches on the Flevoland dataset. It achieves the highest Overall Accuracy (OA = 94%) and Average Accuracy (AA = 93%), demonstrating superior

performance across both homogeneous and heterogeneous land cover classes.

For Simple Classes (Bare Soil, Water), the proposed method achieves 100% accuracy — outperforming all others. Methods like Weighted ML and CLPP-MP also perform well but are less consistent. For Water, the proposed method = 97%, while CLPP-MP = 79%.

For Heterogeneous Classes (Wheat, Beet, Potatoes), the proposed method achieves 90–98% accuracy — the best among all. Weighted KNN and CLPP-GLCM perform well but lag behind in some classes (e.g., beet). For Scattered Classes (Grass, Wheat2, Wheat3), The proposed method achieves 84–95% accuracy — better than CLPP-GLCM and CLPP-MP.

Name of class	Number of training samples	Total samples	Accuracy	Validity
Stembeans	31	6103	0.97	0.97
Peas	46	9111	0.98	0.94
Forest	75	14944	0.96	0.96
Lucerne	48	9477	0.98	0.94
Wheat	87	17283	0.93	0.91
Beet	51	10050	0.89	0.91
Potatoes	77	15292	0.92	0.93
Bare soil	16	3078	1	1
Grass	32	6269	0.81	0.90
Rapeseed	64	12690	0.94	0.89
Barely	36	7156	0.98	0.96
Wheat2	53	10591	0.90	0.97
Wheat3	107	21300	0.96	0.97
Water	68	13476	1	1
Buildings	3	476	0.70	1
Overall accuracy	-	-	92.80	94.95

Table 2. Classification results of the proposed for Flevoland dataset.

Name of class	Number of samples	Number of training samples	CLPP-MP	CLPP-GLCM	CLPP-Gabor	Pol+GLCM	Pol+Gabor	LE-IF	2D-CNN	3D-CNN	Proposed method
mountains	61913	6103	0.82	0.84	0.83	0.64	0.68	0.80	0.18	0.37	0.85
green	135282	9111	0.73	0.73	0.78	0.64	0.63	0.71	0.51	0.44	0.72
water	348639	14944	0.92	0.87	0.87	0.91	0.91	0.88	0.98	0.96	0.99
buildings	375766	9477	0.77	0.67	0.64	0.84	0.83	0.79	0.92	0.96	0.92
Average accuracy	-	-	0.81	0.78	0.78	0.76	0.76	0.80	0.65	0.68	0.88
Overall accuracy	-	-	0.83	0.77	0.76	0.82	0.82	0.82	0.83	0.84	0.91

Table 3. Classification results of the proposed method compared to other methods for San Francisco dataset.

Name of class	Number of training samples	Number of samples	CLPP-MP	CLPP-GLCM	CLPP-Gabor	Weighted KNN	Weighted SVM	Weighted ML	Proposed method
Stembeans	61	6103	0.95	0.87	0.91	0.91	0.93	0.71	0.97
Peas	91	9111	0.98	0.93	0.93	0.92	0.90	0.78	0.98
Forest	149	14944	0.90	0.83	0.83	0.91	0.91	0.76	0.96
Lucerne	94	9477	0.92	0.87	0.86	0.91	0.85	0.94	0.98
Wheat	172	17283	0.98	0.79	0.78	0.82	0.89	0.74	0.93
Beet	100	10050	0.86	0.87	0.93	0.91	0.93	0.46	0.89
Potatoes	152	15292	0.95	0.91	0.94	0.82	0.86	0.83	0.92
Bare soil	30	3078	1	1	1	1	0.98	0.98	1
Grass	62	6269	1	0.77	0.91	0.68	0.81	0.84	0.81
Rapeseed	126	12690	0.95	0.84	0.79	0.79	0.83	0.85	0.94
Barely	71	7156	0.96	0.94	0.96	0.94	0.88	0.91	0.98
Wheat2	105	10591	0.84	0.76	0.80	0.87	0.86	0.88	0.90
Wheat3	213	21300	0.95	0.78	0.88	0.89	0.94	0.91	0.96
Water	134	13476	0.97	0.79	0.79	0.97	0.98	1	1
Buildings	4	476	0.96	0.78	0.77	0.73	0.75	0.23	0.70
Average accuracy	-	-	0.94	0.85	0.87	0.87	0.89	0.79	0.93
Overall accuracy	-	-	0.94	0.84	0.86	0.89	0.93	0.82	0.94

Table 4. Classification results of the proposed method compared to other methods for Flevoland dataset.

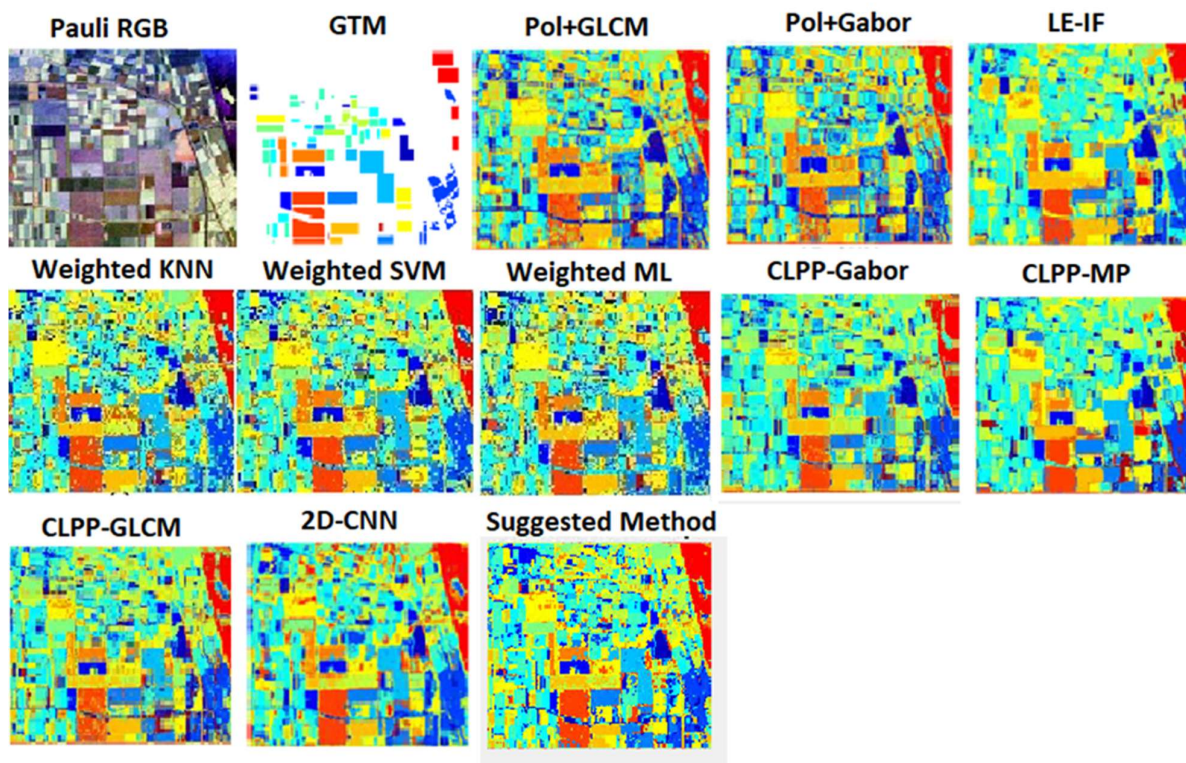


Fig 3. Flevoland classification maps obtained by different methods compared to the proposed method.

4. Conclusion

In this paper, a graph based feature extraction for PolSAR image classification is proposed which in contrast to existing deep learning methods, uses a pre-computed projection matrix as the weight matrix in its propagation rule. The regularized discriminant analysis computed on superpixels is used to provide the pre-computed weight matrix in the graph model. Fusion of graph based features with different combination of scattering features such as entropy, anisotropy and average alpha angle leads to high performance in two benchmark PolSAR datasets.

References

- Alkhatib, M.Q., 2025: PolSAR image classification using complex-valued multiscale attention vision transformer (CV-MSAtViT), *Int. J. Appl. Earth Obs. Geoinf.*, vol. 137, p. 104412, doi: 10.1016/j.jag.2025.104412.
- Bdiri, W., Bouhleb, N., S. Méric, S., Pottier, E., and Kallel, F., 2024: Unsupervised classification of polarimetric SAR images using Bayesian nonparametric model and Markov random field, in *Proc. 32nd Eur. Signal Process. Conf. (EUSIPCO)*, Lyon, France, pp. 2212–2216, doi: 10.23919/EUSIPCO63174.2024.10715374.
- Imani, M., 2021: PolSAR classification using contextual based locality preserving projection and guided filtering, *Int. J. Inf. Commun. Technol. Res.*, vol. 13, no. 2, pp. 29–38.
- Saneipour, F., Imani, M., and Ghassemian, H., 2024: Weighted features based classification of polarimetric SAR images, in *Proc. 13th Iranian and 3rd Int. Conf. Mach. Vis. Image Process. (MVIP)*, Kharazmi Univ., Tehran, Iran, Mar. Paper ID: mvip-1016.
- Bharaneswari, M., Arulmozhivarman, P., Tatavarti, R., and Senthilnathan, K., 2015: Speckle noise suppression in SAR images (Oil spill images) using wavelet based methods and ICA technique, *IEEE International Conference on Signal Processing, Informatics, Communication and Energy Systems (SPICES)*, Kozhikode, India, pp. 1-5.
- Chitroub, S., 2004., PCA-ICA neural network model for POLSAR images analysis, *IEEE International Conference on Acoustics, Speech, and Signal Processing*, Montreal, QC, Canada, 2004, pp. V-757.
- Imani, M., 2022: Entropy/Anisotropy/Alpha Based 3DGabor Filter Bank for PolSAR Image Classification, *Geocarto International*, vol. 37, no. 27, pp. 18491–18519.
- Huang, X., Nie, X., and Qiao, H., 2020: PolSAR Image Feature Extraction Based on Co-Regularization, *IGARSS 2020 - 2020 IEEE International Geoscience and Remote Sensing Symposium*, Waikoloa, HI, USA, pp. 2727-2730.
- Zhang, Q., He, C., He, B., and Tong, M., 2023: Learning Scattering Similarity and Texture-Based Attention With Convolutional Neural Networks for PolSAR Image Classification, in *IEEE Transactions on Geoscience and Remote Sensing*, vol. 61, pp. 1-19.
- Imani, M., 2022: Nearest Polarimetric and Spatial Neighbours for Feature Space Projection and Guidance Image-Based Spatial Filtering for PolSAR Image Classification, *Remote Sensing Letters*, vol. 13, no. 4, pp. 406–417.
- Ni, J., Zhang, F., Ma, F., Yin, Q., and Xiang, D., 2021: Random Region Matting for the High-Resolution PolSAR Image Semantic Segmentation, in *IEEE Journal of Selected Topics in Applied Earth Observations and Remote Sensing*, vol. 14, pp. 3040-3051.
- Wang, Z., Chen, L., Shi, H., Qi, B., Wang, G., 2019: SAR image classification method based on Gabor feature and KNN, "Vol. 2019 Iss. 20, pp. 6734-6736.
- Wang, X., Cao, Z., and Pi, Y., 2022: Semisupervised Classification With Adaptive Anchor Graph for PolSAR Images, in *IEEE Geoscience and Remote Sensing Letters*, vol. 19, pp. 1-5, Art no. 4009705.
- Nie, X., Gao, R., Wang, R., and Xiang, D., 2021: Online Multiview Deep Forest for Remote Sensing Image Classification via Data Fusion, in *IEEE Geoscience and Remote Sensing Letters*, vol. 18, no. 8, pp. 1456-1460.
- Sharma, R., and Panigrahi, R.K., 2021: Texture Classification-Based NLM PolSAR Filter, in *IEEE Geoscience and Remote Sensing Letters*, vol. 18, no. 8, pp. 1396-1400.
- Guo, J., Wang, L., Zhu, D., and Zhang, G., 2022: Semisupervised Classification of PolSAR Images Using a Novel Memory Convolutional Neural Network, in *IEEE Geoscience and Remote Sensing Letters*, vol. 19, pp. 1-5, Art no. 4007605.
- Wang, Y., Cheng, J., Zhou, Y., Zhang, F., and Yin, Q., 2022: A Multichannel Fusion Convolutional Neural Network Based on Scattering Mechanism for PolSAR Image Classification, in *IEEE Geoscience and Remote Sensing Letters*, vol. 19, pp. 1-5, Art no. 4007805.
- Cao, Y., Wu, Y., Li, M., Zheng, M., Zhang, P., and Wang, J., 2023: Multifrequency PolSAR Image Fusion Classification Based on Semantic Interactive Information and Topological Structure, in *IEEE Transactions on Geoscience and Remote Sensing*, vol. 61, pp. 1-15, Art no. 5205715.
- Zhang, F., Li, P., Zhang, Y., Liu, X., Ma, X., and Yin, Z., 2023: A Enhanced DeepLabv3+ for PolSAR image classification, *4th International Conference on Computer Engineering and Application (ICCEA)*, Hangzhou, China, pp. 743-746.

Yin, Q., Lin, Z., Hu, W., López-Martínez, C., Ni, J., and Zhang, F., 2023: Crop Classification of Multitemporal PolSAR Based on 3-D Attention Module With ViT, in IEEE Geoscience and Remote Sensing Letters, vol. 20, pp. 1-5, Art no. 4005405.

Imani, M., 2022: Median-Mean Line Based Collaborative Representation for PolSAR Terrain Classification, The Egyptian Journal of Remote Sensing and Space Sciences, vol. 25, pp. 281–288.

Mou, L., Lu, X., Li, X., and Zhu, X.X., 2020: Nonlocal Graph Convolutional Networks for Hyperspectral Image Classification, IEEE Transactions on Geoscience and Remote Sensing, vol. 58, no. 12, pp. 8246-8257.